Semiconductor Physics, Quantum Electronics & Optoelectronics, 2024. V. 27, No 2. P. 157-161.

Semiconductor physics

Quantum features of low-energy photoluminescence of aluminum nitride films

G.V. Milenin[1], R.A. Redko[1,2]

[1]V. Lashkaryov Institute of Semiconductor Physics, National Academy of Sciences of Ukraine
41, prospect Nauky, 03028 Kyiv, Ukraine
[2]State University of Information and Communication Technologies, 7, Solomenska str., 03110 Kyiv, Ukraine
E-mail: milenin.gv@gmail.com; redko.rom@gmail.com

Abstract. Photoluminescence of aluminum nitride films at the below bandgap excitation has been studied. It has been found that low-energy (up to 2.02 eV) photoluminescence spectra of the AlN films contain a series of equidistant maxima, the intensities of which decrease with energy. Theoretical analysis has shown that the observed photoluminescence features may be caused by strong electron-phonon interaction (long-range interaction of electrons in the band gap with Al^{3+} ions in the lattice sites). This interaction presumably leads to appearance of quasi-particles in the band gap of AlN, which are a bound state of an electron with an ion in a crystal lattice site. Such quasi-particles have been called "elions". The energy of an elion is quantized. An elion quantum is equal to the longitudinal optical phonon energy. The low-energy photoluminescence is based on the elion generation and subsequent annihilation mechanism.

Keywords: aluminum nitride, photoluminescence, electron-phonon interaction, bound state of electron and ion, quasi-particle, elion.

https://doi.org/10.15407/spqeo27.02.157
PACS 61.72.uj, 63.20.kd, 78.55.Cr

Manuscript received 20.03.24; revised version received 18.04.24; accepted for publication 19.06.24; published online 21.06.24.

1. Introduction

In recent years, significant breakthrough in formation of aluminum nitride has been achieved [1–3]. Fabrication of AlN films and nanostructures with good crystalline quality has significant importance for practical application. Due to the wide bandgap of AlN, AlN-based high electron mobility transistors (HEMTs) have been considered for operations at high breakdown voltages under high-temperature conditions [4]. Choice of substrate for growing AlN films depends on the main purpose. Sapphire [5–7], SiC [8], GaN [9, 10] and Si [11, 12] substrates are suitable. The conditions of film fabrication significantly affect the film structural perfection and the quality of the phase interface. Even with a relatively simple DC reactive sputtering system, high-quality AlN films with smooth morphology (0.36 nm) and high crystalline quality can be produced at appropriate Ar/N_2 flow ratio, sputtering power and process pressure [13]. However, the problem of defects in the AlN films still remains actual. Native defects and/or impurities usually cause optical transitions below the bandgap revealed in the absorption and luminescence spectra. Background impurities, such as silicon, carbon, and oxygen lead to additional complexity and formation of specific defect centers. Due to the growing features, oxygen is the dominant impurity in AlN films. Despite numerous experimental works aimed at unveiling the origin of photoluminescence bands in AlN [13, 14], the nature of the radiative recombination in the infrared spectral region, which is observed very rarely [15], is still under debate.

2. Experimental

AlN films were grown by high-frequency reactive magnetron sputtering of an Al target in a 1:3.5 gas mixture of Ar and N_2 using an upgraded industrial setup "Katod 1M". An industrial frequency of 13.56 MHz was used. Before the growing process, the operation volume was pumped out to a pressure of $1.33 \cdot 10^{-3}$ Pa (10^{-5} Torr) by using an oil-free turbomolecular pump TM-1000. The total operation pressure in the chamber during the process was 5.6 Pa ($4 \cdot 10^{-2}$ Torr). PL spectra in the 350…650 nm wavelength range were measured at room temperature at out-of-band excitation using a Perkin-Elmer LS55 PL luminescence spectrometer. The measurement error was below 0.5 nm at the excitation light wavelength of 220 and 250 nm.

3. Results and theoretical analysis

3.1. Results of radiative recombination measurements

Photoluminescence spectra of the AlN films at different excitation levels are shown in Fig. 1. Decrease of the excitation wavelength from 250 to 220 nm results in more distingue of overlapped bands. The bands in the blue region are observed very often [14, 16], hence, we will not consider them in this paper. A characteristic feature of the measured spectra is that a series of equally spaced PL intensity maxima is observed in the energy range up to 2.02 eV (since the band gap of AlN is 6.2 eV, this part of the PL spectra will be called low-energy photoluminescence hereafter). The energy distance between the neighboring maxima is about 0.13 eV. A peculiarity of these maxima is that their intensity values decrease with energy.

3.2. Theoretical analysis

Aluminum nitride is a wide band gap ionic crystal. Al^{3+} and N^{3-} ions are located in the lattice sites. As a result, an electron moving in the crystal interacts with lattice ions and causes displacement of ions with different charges in opposite directions, as in optical vibrations. Such an ion displacement is equivalent to the excitation of longitudinal optical phonons. Consequently, in ionic crystals, electrons effectively interact with longitudinal optical phonons. The coupling constant of electrons with optical phonons (Fröhlich constant) λ is determined by the following formula [17]:

$$\lambda = \frac{e^2}{2\eta\omega_{LO}\left(\eta/2m_n\omega_{LO}\right)^{1/2}} \frac{1}{4\pi\varepsilon_0}\left(\frac{1}{\varepsilon_\infty}-\frac{1}{\varepsilon_S}\right), \qquad (1)$$

where e is the electron charge, $\hbar$ – Planck constant, ε_0 – electrical constant, ω_{LO} – longitudinal optical phonon frequency, m_n – effective electron mass, and ε_s and ε_∞ are the static and high-frequency permittivities, respectively.

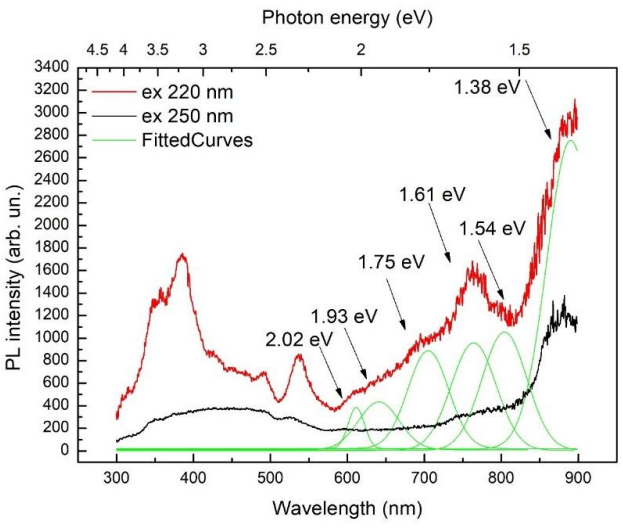

Fig. 1. PL spectra of an AlN film. Green bands are obtained using deconvolution into Gaussians.

We estimate the value of λ for AlN single crystals based on the following known parameters: $m_n = 0.4m_0$, $\hbar\omega_{LO} = 0.0992$ eV, $\varepsilon_s = 8.5$, and $\varepsilon_\infty = 4.6$. From the relation (1), we obtain $\lambda = 0.74$. At equal all the rest parameters, the coupling constant of electrons with optical phonons λ is determined by the values of ε_s and ε_∞. In their turn, the latter values strongly depend on the conditions and methods of deposition of AlN films and, hence, on their structure. In particular, the following values of the static and high-frequency permittivity of the AlN films deposited on a Si substrate are given in [18]: $\varepsilon_s = 11.5$ and $\varepsilon_\infty = 2.94$. With unchanged other parameters, we have $\lambda = 1.9$. In [19], $\varepsilon_s = 20.7$ and $\varepsilon_\infty = 1.2$ were obtained, and $\lambda = 5.8$ in this case.

Thus, $\lambda > 1$ for AlN films and can even reach the values characteristic of alkali-halide crystals ($6.4 > \lambda > 4.8$). That is, a strong electron-phonon interaction is observed. Therefore, for the AlN films with strong electron-phonon interaction, interaction of non-equilibrium (excited by electromagnetic radiation) electrons with the ionic subsystem of the crystal during the electron relaxation must be taken into account.

Ions in the lattice sites perform harmonic oscillations. Such an oscillatory system in a three-dimensional crystal (each ion has three degrees of freedom) is a superposition of $3N$ normal vibrations (optical and acoustic, N longitudinal and 2 transverse ones), where N is the number of ions in the crystal. When the numbers of the longitudinal optical and acoustic vibrations are the same, the number of the longitudinal optical vibrations is $N/2$. Each normal vibration is a quantum harmonic oscillator. The energy levels of a quantum harmonic oscillator with a frequency ω_{LO} are expressed by the following relation [20, 21]:

$$E_n = \eta\omega_{LO}\left(n+\frac{1}{2}\right), \qquad (2)$$

where n is the quantum number that takes the values 0, 1, 2, 3, ….

Strong electron-phonon interaction means that the electronic and ionic subsystems of the crystal are strongly coupled. In this particular case, the strong electron-phonon interaction is caused by the strong long-range interaction of electrons in the band gap with triply charged Al cations in the lattice sites. This results in formation of a quasi-particle, which is a bound state of an electron and an ion (e^- – Al^{3+}) in the band gap. We call this quasi-particle an “elion”. As already mentioned above, ions in the lattice sites are quantum harmonic oscillators. The energy of an ion, which is the heaviest component of the bound state of an electron with the ion, is quantized. The difference in the energies between the neighboring levels is equal to the longitudinal optical phonon energy $\hbar\omega_{LO}$ (formula (2)). Therefore, the energy of an elion is also quantized. The elion quantum is numerically equal to the longitudinal optical phonon energy. Consequently, the expression (2) describes the system of the energy levels of an elion, which are equivalent to the levels of a quantum harmonic oscillator

(the energy of the levels is counted from the top of the valence band). Note that for a quantum harmonic oscillator, only transitions between neighboring levels are possible: $\Delta n = \pm 1$. However, electron in the elion is not a quantum harmonic oscillator as such, since its oscillations are induced by motion of another component of the quasi-particle – the ion. Therefore, radiative transitions of electrons do not obey this selection rule. Such transitions can take place from any level of the elion to the valence band.

We suggest therefore that the mechanism of radiative recombination in a certain energy range in the AlN films is caused by generation of elions under the action of electromagnetic radiation and their subsequent annihilation as a result of transitions of non-equilibrium electrons from the energy levels of the quasi-particle to the valence band. Let us determine the range of the elion energy spectrum. The probability P_n of a quantum harmonic oscillator under thermal equilibrium at a temperature T to be in the state E_n is [21]

$$P_n = A\exp\left(-\frac{E_n}{kT}\right), \quad (3)$$

where A is the coefficient determined from the probability normalization condition:

$$\sum_n P_n = 1. \quad (4)$$

The relation for A has the following form [21]:

$$A = \exp\left(\frac{\eta\omega_{LO}}{2kT}\right)\left[1-\exp\left(-\frac{\eta\omega_{LO}}{kT}\right)\right]. \quad (5)$$

For an ensemble of $N/2$ oscillators that do not interact with each other, the quantity D_n of the oscillators in the n state is

$$D_n = \frac{1}{2}NP_n. \quad (6)$$

Combining (3), (5) and (6) gives

$$D_n = \frac{1}{2}N\exp\left(\frac{\eta\omega_{LO}}{2kT}\right)\left[1-\exp\left(-\frac{\eta\omega_{LO}}{kT}\right)\right]\exp\left(-\frac{E_n}{kT}\right). \quad (7)$$

For two ensembles of $N/2$ quantum harmonic oscillators and $N_e/2$ non-equilibrium electrons excited by electromagnetic radiation (2 in the denominator means that two electrons with opposite spins may be at the same energy level), the product Π of the number of electrons $N_e/2$ and the number of oscillators D_n in the n state is equal to

$$\Pi = \frac{1}{4}NN_e\exp\left(\frac{\eta\omega_{LO}}{2kT}\right)\left[1-\exp\left(-\frac{\eta\omega_{LO}}{kT}\right)\right]\exp\left(-\frac{E_n}{kT}\right). \quad (8)$$

The product Π characterizes the population of the levels E_n with non-equilibrium electrons. We assume that the maximum value of the energy $E_{n\max}$ of the spectrum of electron levels in the band gap is found from the condition $\Pi = 1$ and equals as

$$E_{n\max} = kT\ln\left\{\frac{1}{4}NN_e\exp\left(\frac{\eta\omega_{LO}}{2kT}\right)\left[1-\exp\left(-\frac{\eta\omega_{LO}}{kT}\right)\right]\right\}. \quad (9)$$

As follows from (9), $E_{n\max}$ depends on the values of ω_{LO} and N_e. When all the N^{3-} ions in the crystal, which is the half of the total number of ions, are ionized by electromagnetic radiation, the number of electrons is equal to $N_e = N/2$. In its turn, the number of ions is determined by the crystal film volume excited by radiation, *i.e.* it is equal to the product of the ion concentration and the film volume. Finally, we have

$$E_{n\max} = kT\ln\left\{\frac{1}{8}N^2\exp\left(\frac{\eta\omega_{LO}}{2kT}\right)\left[1-\exp\left(-\frac{\eta\omega_{LO}}{kT}\right)\right]\right\}. \quad (10)$$

As noted above, we call the photoluminescence of AlN in the energy range up to $E_{n\max}$ the low-energy one.

Therefore, a series of peaks in the PL spectrum of AlN in the range of photon energies $\eta\omega \le E_{\max}$ may be caused by generation of elions due to strong electron-phonon interaction and their subsequent annihilation. As the energy increases, the intensity of the PL peaks should decrease due to the decrease in the population of the energy levels (2) with phonons and, hence, with electrons.

Now we calculate the constant of electron-phonon interaction λ, spectrum of energy levels E_n and maximum value $E_{\max}$ for the AlN films under investigation.

Based on the transmission spectra and electro-physical measurements of the AlN films [22, 23], the following values for the frequency of transverse optical phonons ω_{TO} as well as the ratio of the dielectric permittivities were obtained: $\omega_{TO} = 1.35\cdot10^{14}$ rad·s^{-1} and $\varepsilon_s/\varepsilon_\infty = 2.15$. Using the Lidden–Sachs–Teller relation, we obtain that the frequency of longitudinal optical phonons is $\omega_{LO} = 1.98\cdot10^{14}$ rad·s^{-1}. Accordingly, $\hbar\omega_{LO} = 0.13$ eV. This value exceeds the one for AlN single crystals, which may be caused by presence of defects in the films.

The AlN films had a thickness of $3\cdot10^{-6}$ m. The illuminated surface area of the films during measurements of the PL spectra was about $7\cdot10^{-6}$ m^2. The number of ions per unit volume in AlN is $9.28\cdot10^{28}$ m^{-3}. Then $N = 1.95\cdot10^{18}$ and, according to (10), $E_{n\max} = 2.17$ eV at $T = 298$ K. The spectrum of the electron energy levels E_n calculated by (2) and the experimentally observed positions of the PL intensity maxima E_{PL} in the phonon energy scale are presented in Table.

Table. Theoretical and experimental values of the positions of the PL intensity maxima.

n	E_n, eV	E_{PL}, eV
10	1.37	1.38
11	1.50	1.54
12	1.63	1.61
13	1.76	1.75
14	1.89	1.93
15	2.02	2.02

Hence, the proposed theoretical analysis of the quantum nature of spectrum of the low-energy photoluminescence of AlN films made it possible to substantiate both the energy positions of the maxima and the change in their values with energy. The features of the PL spectrum at the energies above 2.2 eV are caused by defects in the AlN film structure.

4. Conclusions

The intensity distribution in the low-energy photoluminescence spectra of aluminum nitride films contains a series of maxima spaced from each other by the same energy value equal to the longitudinal optical phonon energy. As the energy increases, the maximum values of the PL intensity decrease.

A theoretical justification for the observed phenomena has been proposed. It is based on the assumption that strong electron-phonon interaction in the band gap of the AlN films leads to formation of quasi-particles, which are bound states of an electron and an ion (e^- – Al^{3+}). These quasi-particles have been called "elions". The elion energy is quantized. The quantum is numerically equal to the energy of longitudinal optical phonons.

Therefore, low-energy radiative recombination may be explained by the mechanism of formation and subsequent annihilation of elions. The energy interval between the neighboring maxima of PL intensity is equal to the elion quantum. With increasing the energy, the intensity of the PL peaks decreases due to a decrease in the population of the energy levels with phonons and, hence, with electrons.

Acknowledgment

This work was supported by the National Research Foundation of Ukraine (Project No. 2022.01/0126).

Reference

1. Singh P.D.D., Murthy Z.V.P., Kailasa S.K. Metal nitrides nanostructures: Properties, synthesis and conceptualization in analytical methods developments for chemical analysis and separation, and in energy storage applications. *Coord. Chem. Rev*. 2023. **481**. P. 215046. https://doi.org/10.1016/j.ccr.2023.215046.
2. Sager A., Esen I., Ahlatçi H., Turen Y. Characterization and corrosion behavior of composites reinforced with ZK60, AlN, and SiC particles. *Eng. Sci. Technol*. 2023. **41**. P. 101389. https://doi.org/10.1016/j.jestch.2023.101389.
3. McLeod A.J., Ueda S.T., Lee P.C. *et al.* Pulsed chemical vapor deposition for crystalline aluminum nitride thin films and buffer layers on silicon and silicon carbide. *Thin Solid Films*. 2023. **768**. P. 139717. https://doi.org/10.1016/j.tsf.2023.139717.
4. Namikawa G., Shojiki K., Yoshida R. *et al.* MOVPE growth of AlN and AlGaN films on N-polar annealed and sputtered AlN templates. *J. Cryst. Growth*. 2023. **617**. P. 127256. https://doi.org/10.1016/j.jcrysgro.2023.127256.
5. Tanaka S., Shojiki K., Uesugi K. *et al.* Quantitative evaluation of strain relaxation in annealed sputter-deposited AlN film. *J. Cryst. Growth*. 2019. **512**. P. 16–19. https://doi.org/10.1016/j.jcrysgro.2019.02.001.
6. Shojiki K., Uesugi K., Kuboya S., Miyake H. Reduction of threading dislocation densities of N-polar face-to-face annealed sputtered AlN on sapphire. *J. Cryst. Growth*. 2021. **574**. P. 126309. https://doi.org/10.1016/j.jcrysgro.2021.126309.
7. Miyake H., Lin C.-H., Tokoro K., Hiramatsu K. Preparation of high-quality AlN on sapphire by high-temperature face-to-face annealing. *J. Cryst. Growth*. 2016. **456**. P. 155–159. https://doi.org/10.1016/j.jcrysgro.2016.08.028.
8. Lemettinen J., Chowdhury N., Okumura H. *et al.* Nitrogen-polar polarization-doped field-effect transistor based on $Al_{0.8}Ga_{0.2}N$/AlN on SiC with drain current over 100 mA/mm. *IEEE Electron. Device Lett.* 2019. **40**. P. 1245–1248. https://doi.org/10.1109/LED.2019.2923902.
9. Sobczak K., Borysiuk J., Strąk P. *et al.* Detection of Si doping in the AlN/GaN MQW using Super X – EDS measurements. *Micron*. 2020. **134**. P. 102864. https://doi.org/10.1016/j.micron.2020.102864.
10. Ramesh R., Arivazhagan P., Prabakaran K. *et al.* Influence of AlN interlayer on AlGaN/GaN heterostructures grown by metal organic chemical vapour deposition. *Mater. Chem. Phys.* 2021. **259**. P. 124003. https://doi.org/10.1016/j.matchemphys.2020.124003.
11. Chen W.-C., Chen H.-P., Lin Y.-W., Liu D.-R. Growth of narrow substrate temperature window on the crystalline quality of InN epilayers on AlN/Si(111) substrates using RF-MOMBE. *J. Cryst. Growth*. 2019. **522**. P. 204–209. https://doi.org/10.1016/j.jcrysgro.2019.06.031.
12. Kumar K., Kumar A., Kaur D. Improved power conversion efficiency in *n*-MoS_2/AlN/*p*-Si (SIS) heterojunction based solar cells. *Mater. Lett.* 2020. **277**. P. 128360. https://doi.org/10.1016/j.matlet.2020.128360.
13. Liu H., Guo W. The interplay of process parameters and influence on the AlN films on sapphire fabricated by DC magnetron sputtering and annealing. *Semicond. Sci. Technol.* 2023. **38**. P. 015020. https://doi.org/10.1088/1361-6641/aca8ca.
14. Koppe T., Hofsäss H., Vetter U. Overview of band-edge and defect related luminescence in aluminum nitride. *J. Lumin*. 2016. **178**. P. 267–281. https://doi.org/10.1016/j.jlumin.2016.05.055.
15. Zhou Q., Zhang Z., Li H. *et al.* Below bandgap photoluminescence of an AlN crystal: Co-existence of two different charging states of a defect center. *APL Mater*. 2020. **8**. P. 081107. https://doi.org/10.1063/5.0012685.

16. Kai C., Zang H., Ben J. *et al.* Origination and evolution of point defects in AlN film annealed at high temperature. *J. Lumin*. 2021. **235**. P. 118032. https://doi.org/10.1016/j.jlumin.2021.118032.
17. Germain M., Kartheuser E., Gurskii A.L. *et al.* Effects of electron–phonon interaction and chemical shift on near-band-edge recombination in GaN. *J. Appl. Phys.* 2002. **91**. P. 9827–9834. https://doi.org/10.1063/1.1471368.
18. Sudzhanskaya I.V., Kolesnikov D.A., Beresnev V.M. *et al.* Properties of AlN coating reseived by vacuum-arc method on silicon. *Problems of Atomic Science and Technology*. 2011. No 6. P. 145–148.
19. Bi Z.X., Zheng Y.D., Zhang R. *et al.* Dielectric properties of AlN film on Si substrate. *J. Mater. Sci.: Mater. Electron*. 2004. **15**. P. 317–320. https://doi.org/10.1023/B:JMSE.0000024233.82681.dc.
20. Griffiths D.J., Schroeter D.F. *Introduction to Quantum Mechanics*. Cambridge University Press, Cambridge, 2018.
21. Kittel C. *Introduction to Solid State Physics*. John Wiley & Sons, Inc, 2004.
22. Zayats N.S., Boiko V.G., Gentsar P.A. *et al*. Optical studies of AlN/*n*-Si(100) films obtained by the method of high-frequency magnetron sputtering. *Semiconductors*. 2008. **42**. P. 195–198. https://doi.org/10.1134/S1063782608020139.
23. Zayats M.S., Boiko V.G., Romanyuk B.M., Lytvyn P.M. Low-temperature ion-plasma technology of deposition of nanostructured films of aluminum and boron nitrides. *Optoelectron. Semicond. Tech*. 2021. **56**. P. 97–107.

Authors and CV

Milenin G.V. PhD in Solid-State Physics, Senior Researcher at the V. Lashkaryov Institute of Semiconductor Physics, NASU. Authored and co-authored more than 90 scientific publications, 2 monographs, and 6 patents. The area of his scientific interests is semiconductor physics and solid-state electronics. https://orcid.org/0000-0002-1971-9571

Redko R.A. PhD in Solid-State Physics, Acting Scientific Secretary of the V. Lashkaryov Institute of Semiconductor Physics, NASU. Associate Professor at the State University of Information and Communication Technologies. Authored and co-authored more than 90 scientific publications, 1 monograph, and 6 patents. The area of his scientific interests is semiconductor physics and solid-state electronics.
https://orcid.org/0000-0001-9036-5852

Authors' contributions

Milenin G.V.: conceptualization, writing – original draft, validation, methodology, writing – review & editing.

Redko R.A.: investigation, validation, methodology , writing – review & editing.

Квантові особливості низькоенергетичної фотолюмінесценції плівок нітриду алюмінію

Г.В. Міленін, Р.А. Редько

Анотація. Досліджено фотолюмінесценцію плівок нітриду алюмінію при збудженнях, що знаходяться нижче забороненої зони. Встановлено, що низькоенергетичний спектр фотолюмінесценції плівок нітриду алюмінію (в області енергій до 2,02 еВ включно) являє собою серію рівновіддалених один від одного максимумів, значення інтенсивності яких зменшуються зі збільшенням енергії. Теоретичний аналіз показав, що зазначені особливості явищ фотолюмінесценції можуть бути спричинені сильною електрон-фононною взаємодією (сильна далека взаємодія електрона в забороненій зоні з тризарядними позитивно зарядженими іонами алюмінію (Al^{3+}) у вузлах ґратки). Ця взаємодія, імовірно, приводить до появи квазічастинки в забороненій зоні нітриду алюмінію – зв'язаного стану електрона з іоном у вузлі кристалічної ґратки. Цей квантовий об'єкт отримав назву «еліон». Енергія еліона квантована. Квант еліона дорівнює енергії поздовжнього оптичного фонона. В основі низькоенергетичної фотолюмінесценції лежить механізм генерації та подальшої анігіляції еліонів.

Ключові слова: нітрид алюмінію, фотолюмінесценція, електрон-фононна взаємодія, зв'язаний стан електрона та іона, квазічастинка, еліон.